

# Growth and spectral properties of $\text{Er}^{3+}/\text{Yb}^{3+}:\text{Li}_3\text{Ba}_2\text{Gd}_3(\text{WO}_4)_8$ crystal

YUNXIA ZHAO<sup>a,b</sup>, YISHENG HUANG<sup>a</sup>, LIZHEN ZHANG<sup>a</sup>, ZHOUBIN LIN<sup>a</sup>, GUOFU WANG<sup>a,\*</sup>

<sup>a</sup>Key Laboratory of Optoelectronics Material Chemistry and Physics, Fujian Institute of Research on the Structure of Matter, Chinese Academy of Sciences, Fuzhou, Fujian 350003, China

<sup>b</sup>Graduate School of Chinese Academy of Sciences, Beijing 100037, China

$\text{Er}^{3+}/\text{Yb}^{3+}:\text{Li}_3\text{Ba}_2\text{Gd}_3(\text{WO}_4)_8$  crystal has been grown by the top-seeded solution growth (TSSG) method using flux of  $\text{Li}_2\text{WO}_4$ . The polarized spectroscopic properties of  $\text{Er}^{3+}/\text{Yb}^{3+}:\text{Li}_3\text{Ba}_2\text{Gd}_3(\text{WO}_4)_8$  crystal were investigated. Based on the Judd-Ofelt theory, the oscillator strength parameters, spontaneous emission probability, fluorescence branching ratio as well as radiative lifetime were estimated. The up-conversion fluorescence spectrum and mechanism were also discussed. The spectroscopic analysis reveals that  $\text{Er}^{3+}/\text{Yb}^{3+}:\text{Li}_3\text{Ba}_2\text{Gd}_3(\text{WO}_4)_8$  crystal may become a potential candidate for solid-state laser gain medium material.

(Received February 22, 2012; accepted April, 11, 2012)

**Keywords:** Growth,  $\text{Eu}^{3+}$  doped crystal luminescence

## 1. Introduction

Much research attention has been focus on the  $\text{Er}^{3+}$  doped materials [1-5] due to its plenty energy levels producing transitions at various wavelength from visible region at  $\sim 550$  nm (due to  $^4\text{S}_{3/2} \rightarrow ^4\text{I}_{15/2}$  transition) to near-infrared region at  $\sim 1.55\mu\text{m}$  ( $^4\text{I}_{13/2} \rightarrow ^4\text{I}_{15/2}$  transition) and at  $\sim 3\mu\text{m}$  ( $^4\text{I}_{11/2} \rightarrow ^4\text{I}_{13/2}$  transition). The  $\text{Er}^{3+}$  ion has two absorption bands at around 980 nm ( $^4\text{I}_{15/2} \rightarrow ^4\text{I}_{11/2}$  transition) and 810 nm ( $^4\text{I}_{15/2} \rightarrow ^4\text{I}_{9/2}$  transition), which coincides with wavelength of radiation from AlGaAs and InGaAs diode laser. Therefore, the  $\text{Er}^{3+}$ -doped crystals are promising materials for diode pumped solid lasers. The wavelength of 1.55  $\mu\text{m}$  laser is eye safe and has numerous applications such as optical communication, medicine ranging and so on [6-9]. Since the  $\text{Yb}^{3+}$  ion has a broad and high absorption band around 980 nm and can easily pumped with diode laser. When the  $\text{Yb}^{3+}$  and  $\text{Er}^{3+}$  ions were co-doped materials, the  $\text{Yb}^{3+}$  can reduce the lasing threshold and improve the absorption efficiency of erbium laser, such as  $\text{Er}^{3+}/\text{Yb}^{3+}:\text{YVO}_4$  [9],  $\text{Er}^{3+}/\text{Yb}^{3+}:\text{Ca}_3\text{Ln}_2(\text{BO}_3)_4$  ( $\text{Ln}=\text{Gd},\text{La}$ ) [10],  $\text{Er}^{3+}/\text{Yb}^{3+}:\text{YAB}$  [2].

$\text{Li}_3\text{Ba}_2\text{Ln}_3(\text{WO}_4)_8$  ( $\text{Ln}=\text{La}-\text{Lu}, \text{Y}$ ) belongs to the monoclinic system with space group  $C2/c$ , which was firstly discovered by our group [11]. The absorption and emission spectral bands of these family crystals broadened are due to its structural disordering, and they possess a number of advantages as a active media in LD-pumped solid-state lasers [11, 12]. In this work, we report the growth and polarized spectroscopic properties as well as the up-conversion mechanism of the  $\text{Er}^{3+}/\text{Yb}^{3+}:\text{Li}_3\text{Ba}_2\text{Gd}_3(\text{WO}_4)_8$ .

## 2. Experiment

### 2.1 Crystal growth

Since  $\text{Li}_3\text{Ba}_2\text{Gd}_3(\text{WO}_4)_8$  (LBGW) crystal melts incongruently at high temperature, single crystal of  $\text{Er}^{3+}/\text{Yb}^{3+}$ -doped  $\text{Li}_3\text{Ba}_2\text{Gd}_3(\text{WO}_4)_8$  ( $\text{Er}/\text{Yb}:\text{LBGW}$ ) was grown by the top-seeded solution growth (TSSG) technique from a flux of  $\text{Li}_2\text{WO}_4$ . The chemicals used were  $\text{Li}_2\text{CO}_3$ ,  $\text{BaCO}_3$ ,  $\text{Gd}_2\text{O}_3$ ,  $\text{Er}_2\text{O}_3$ ,  $\text{Yb}_2\text{O}_3$  and  $\text{WO}_3$  with AR grade. The solution composition consisted of 75 mol.%  $\text{Li}_2\text{WO}_4$  and 25 mol.%  $\text{Li}_3\text{Ba}_2\text{Gd}_3(1-x-y)\text{Er}_{3x}\text{Yb}_{3y}(\text{WO}_4)_8$  where the molar ration of  $x:y$  is 1:10. The crystal growth details were followed that of ref 11. A single crystal with dimensions of 32 mm  $\times$  13 mm  $\times$  6 mm was successfully grown from the flux of  $\text{Li}_2\text{WO}_4$  using TSSG method. Fig. 1 shows the as-grown crystal and polished crystal plate used in the spectroscopy study. The LBGW crystal with monoclinic system is optical biaxial, there are three optical indicatrix, one of the principal axis is parallel to the  $b$ -axis, marked as Y; the other two principal axes perpendicular between each other and to  $b$ -axis can be found easily by means of crossed polarized microscopy, marked as X and Y, as shown in Fig. 1. We just distinguish the three optical indicatrix, but can not accurately measure the refractive index, because of the lack of precision of our equipment. In the grown  $\text{Er}/\text{Yb}:\text{LBGW}$  crystal the concentration of  $\text{Er}^{3+}$  ions was determined to be 1.03 at.% ( i. e.  $0.487 \times 10^{20}$  ions/ $\text{cm}^3$ ), and that of  $\text{Yb}^{3+}$  ions was determined to be 3.78 at.% ( i. e.  $1.779 \times 10^{20}$  ions/ $\text{cm}^3$ ) by the inductively coupled plasma atom emission spectrometry (ICP-AES).

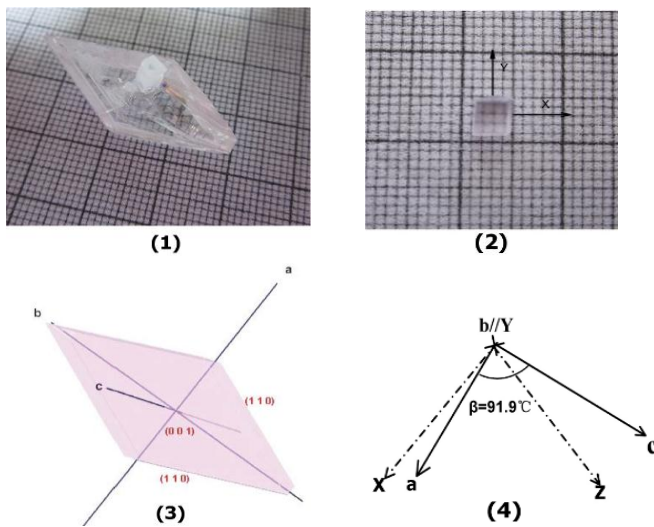


Fig. 1. (1) As grown Er/Yb:LBGW single crystal; (2) A slice cut and perpendicular to the Z-axis; (3) Simulated morphology scheme of the crystal; (4) Relation between optical indicatrix and crystallographic axis.

## 2.2 Spectral measurements

The polarized absorption spectra were recorded using a Perkin-Elmer UV-VIS-NIR spectrometer (Lamada-900) in range of 300-1650 nm. The polarized fluorescence spectra were recorded by a spectrophotometer (FLS920, Edinburgh) equipped with a laser diode (LD) as the excitation source. Furthermore, the up-conversion spectroscopic experiments were carried out by a monochromator (Triax550, Jobin-Yvon) excited at 980nm with a laser diode (LD) and the power range of the diode emission was from 100 mW to 1200 mW. The signals were detected with a PMT (R943-02, Hamamasu). In the experiment all measurements were performed at room temperature, and the light-vector is parallel to X-, Y-, and Z- principal optical directions, respectively.

## 3. Results and discussion

### 3.1 Absorption spectrum and Judd-Ofelt Analysis

Fig. 2 shows the polarized absorption spectrum of Er/Yb:LBGW crystal at room temperature. Eleven

absorption bands are observed. The absorption band around 900-1050nm is due to both  $^4I_{15/2} \rightarrow ^4I_{11/2}$  transition of  $Er^{3+}$  ion and  $^2F_{7/2} \rightarrow ^2F_{5/2}$  transition of  $Yb^{3+}$  ion, the other bands are related to the transitions of  $Er^{3+}$  ion from the  $^4I_{15/2}$  ground multiplet to excited multiplets, 366 ( $^4G_{9/2}$ ), 380 ( $^4G_{11/2}$ ), 408 ( $^2G_{9/2}$  and  $^4F_{9/2}$ ), 453 ( $^4F_{3/2}$  and  $^4F_{5/2}$ ), 490 ( $^4F_{7/2}$ ), 522 ( $^2H_{11/2}$ ), 545 ( $^4S_{3/2}$ ), 657 ( $^4F_{9/2}$ ), 806 ( $^4I_{9/2}$ ) and 1501 nm ( $^4I_{13/2}$ ). There are 11 obvious absorption bands in all absorption spectra of the three polarized directions. Table 1 shows the peak absorption cross-section  $\sigma_{abs}$  at 978 and 1500 nm, which was determined using the formula  $\sigma_{abs} = a/N_c$ , where  $a$  is absorption coefficient,  $N_c$  is the concentration of  $Er^{3+}$  ions in the Er/Yb:LBGW crystal. The absorption full-width at half maximum (FWHM) are 39, 47 and 59 nm for X-, Y- and Z- optical directions around 980 nm respectively. Such broad absorption band is suitable for InGaAs diode-laser pumping.

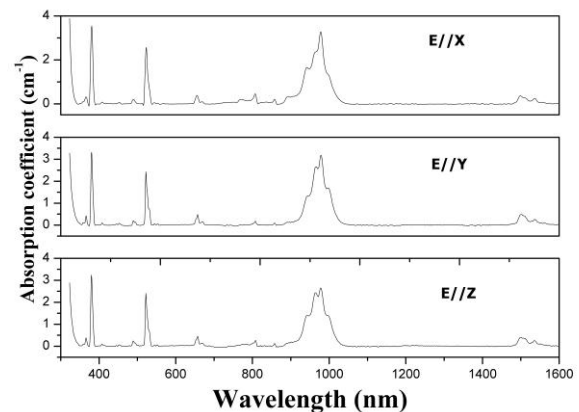


Fig. 2. Polarized absorption spectra of Er/Yb:LBGW crystal at room temperature.

According to the Judd-Ofelt theory [13, 14], the data of the absorption spectrum can be used to predict the oscillator strength parameters, the fluorescence branch ratios, the transition probabilities and radiative lifetime. The calculating procedures follow those described elsewhere [15-20]. The calculated results are listed in Table 2, Table 3 and Table 4.

Table 1. Peak absorption cross-section  $\sigma_{abs}$  for three polarization direction of Er/Yb:LBGW crystal.

Transitions	E//X		E//Y		E//Z	
	$\lambda_{abs}$ (nm)	$\sigma_{abs}(\times 10^{-20} \text{cm}^2)$	$\lambda_{abs}$ (nm)	$\sigma_{abs}(\times 10^{-20} \text{cm}^2)$	$\lambda_{abs}$ (nm)	$\sigma_{abs}(\times 10^{-20} \text{cm}^2)$
$^4I_{15/2} \rightarrow$						
$^4I_{13/2}$	1500	0.82	1500	0.99	1500	0.77
$^4I_{11/2}$	978	1.87	978	1.78	978	1.49

Table 2. Oscillator strength parameters of  $\text{Er}^{3+}$  in  $\text{Er}/\text{Yb}:\text{LBGW}$  crystal.

$\Omega_i$ ( $10^{-20}\text{cm}^2$ )	E//X	E//Y	E//Z	Effective
$\Omega_2$	9.827	8.1008	7.847	8.592
$\Omega_4$	1.993	1.75606	1.862	1.870
$\Omega_6$	0.206	0.319	0.216	0.247

Table 3. Values of measured and calculated oscillator strengths for absorption transitions of  $\text{Er}^{3+}$  in  $\text{Er}/\text{Yb}:\text{LBGW}$  crystal.

Transitions	E//X		E//Y		E//Z	
	$S_{\text{exp}}$	$S_{\text{cal}}$	$S_{\text{exp}}$	$S_{\text{cal}}$	$S_{\text{exp}}$	$S_{\text{cal}}$
$^4\text{I}_{15/2} \rightarrow$						
$^4\text{I}_{13/2}$	6.612e-021(ed)	7.198e-021 (ed)	7.537e-021 1.336e-024 (md)	8.217e-021(ed)	5.692e-021	6.801e-021(ed)
$^4\text{I}_{9/2}$	7.654e-021	3.472e-021	3.489e-021	3.073e-021	4.329e-021	3.246e-021
$^4\text{F}_{9/2}$	8.872e-021	1.162e-020	1.009e-020	1.088e-020	9.372e-021	1.096e-020
$^4\text{S}_{3/2}$	9.84e-022	4.545e-022	2.469e-021	7.068e-022	1.75e-021	4.766e-022
$^2\text{H}_{11/2}$	7.207e-020	7.842e-020	6.033e-020	6.525e-020	5.881e-020	6.379e-020
$^4\text{F}_{7/2}$	5.61e-021	4.249e-021	5.527e-021	4.613e-021	6.033e-021	4.117e-021
$^4\text{F}_{5/2} + ^4\text{F}_{3/2}$	2.591e-021	2.615e-022	1.577e-021	4.066e-022	1.673e-021	2.742e-022
$^2\text{H}_{9/2}$	3.093e-021	8.422e-022	1.384e-021	1.054e-021	2.659e-021	8.398e-022
$^4\text{G}_{11/2}$	1.059e-019	1.009e-019	8.782e-020	8.399e-020	8.598e-020	8.209e-020
$^4\text{G}_{9/2} + ^2\text{K}_{15/2} + ^2\text{G}_{7/2}$	7.505e-021	5.066e-021	5.866e-021	4.635e-021	6.76e-021	4.762e-021
$rms\Delta f$	3.94e-021		2.594e-021		2.912e-021	
$rms\ error(\%)$	8.675		7.633		8.769	

Table 4. Calculated intensity radiative characteristic,  $A_{JJ'}^{ed}$ ,  $A_{JJ'}^{md}$ , and  $A_{JJ'}^{Total}$ ,  $\beta$ , and  $\tau_{rad}$  of  $J \rightarrow J'$  channels of  $\text{Er}^{3+}$  in  $\text{Er}/\text{Yb}:\text{LBGW}$  crystal.

Manifolds		$\lambda$ (nm)	E//X	E//Y	E//Z	$A_{JJ'}^{Total}$ ( $\text{s}^{-1}$ )	$\beta$ (%)	$\tau_{rad}$ (ms)		
$J$	$\rightarrow$		$J'$	$A_{JJ'}^{ed}$ ( $\text{s}^{-1}$ )	$A_{JJ'}^{ed}$ ( $\text{s}^{-1}$ )				$A_{JJ'}^{ed}$ ( $\text{s}^{-1}$ )	$A_{JJ'}^{md}$ ( $\text{s}^{-1}$ )
$^4\text{I}_{13/2}$	$\rightarrow$	$^4\text{I}_{15/2}$	1543	81.00	92.46	76.53	77.53	160.86	100	6.21
$^4\text{I}_{11/2}$	$\rightarrow$	$^4\text{I}_{13/2}$	2746	20.71	21.33	18.92	17.31	37.63	18.1	4.81
		$^4\text{I}_{15/2}$	988	179.61	177.79	153.63		170.34	81.9	
$^4\text{I}_{9/2}$	$\rightarrow$	$^4\text{I}_{11/2}$	4488	1.22	1.17	1.13	2.47	3.64	1.0	2.61
		$^4\text{I}_{13/2}$	1704	20.17	29.36	20.75		23.43	6.1	
		$^4\text{I}_{15/2}$	810	378.60	335.12	353.95		355.89	92.9	
$^4\text{F}_{9/2}$	$\rightarrow$	$^4\text{I}_{9/2}$	3466	17.71	14.67	14.19	5.36	20.88	0.1	0.393
		$^4\text{I}_{11/2}$	1956	75.67	77.39	65.76	12.16	85.1	3.3	
		$^4\text{I}_{13/2}$	1142	162.90	145.20	147.61		151.90	6.0	
		$^4\text{I}_{15/2}$	656	2378.43	2226.89	2244.18		2283.17	89.9	
$^4\text{S}_{3/2}$	$\rightarrow$	$^4\text{F}_{9/2}$	3125	0.29	0.43	0.30		0.34	0.1	1.27
		$^4\text{I}_{9/2}$	1666	65.51	68.75	63.07		65.78	8.4	
		$^4\text{I}_{11/2}$	1215	19.01	25.00	19.15		21.05	2.6	
		$^4\text{I}_{13/2}$	842	172.32	267.95	180.68		206.98	26.5	
		$^4\text{I}_{15/2}$	545	406.59	632.21	426.29		488.36	62.4	

### 3.2 Fluorescence spectra and stimulated emission cross-section

Fig. 3 shows the polarized fluorescence spectra of Er/Yb:LBGW crystal excited by 521 nm radiation at room temperature. Three intensive fluorescence bands centered at 853, 1002 and 1533 nm were observed, corresponding to the  $^4S_{3/2} \rightarrow ^4I_{13/2}$ ,  $^4I_{11/2} \rightarrow ^4I_{15/2}$  and  $^4I_{13/2} \rightarrow ^4I_{15/2}$  transitions, respectively. Fig. 4 shows the polarized fluorescence spectra of Er/Yb:LBGW crystal excited by 980 nm radiation. The emission band of the  $^4I_{13/2} \rightarrow ^4I_{15/2}$  transition of  $Er^{3+}$  has a full-width at half maximum (FWHM) of 65 nm for E//Y polarization, such broad emission band was caused by the disorder structure of the LBGW crystal [11]. The stimulated emission cross-section can be estimated from the fluorescence spectrum by the Fuchtbauer-Ladenburg (F-L) equation [21]:

$$\sigma_{em}(\lambda) = \frac{3\lambda^5 \beta I(\lambda)}{8\pi c n^2 \tau_r \int \lambda [I_x(\lambda) + I_y(\lambda) + I_z(\lambda)] d\lambda} \quad (15)$$

where  $I(\lambda)$  is the fluorescence intensity at wavelength  $\lambda$ ,  $\beta$  is the branching ratio, and  $\tau_r$  is the radiative lifetime. The peak stimulated emission cross-section of Er/Yb:LBGW crystal for the E//Y polarization was calculated to be  $0.61 \times 10^{-20} \text{ cm}^2$  at 1.5  $\mu\text{m}$ , which is comparable to those reported  $Er^{3+}$ -doped materials, for example Er:YAG ( $0.7 \times 10^{-20} \text{ cm}^2$ ) [22].

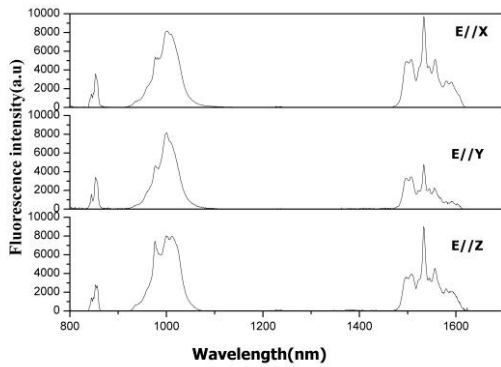


Fig. 3. Polarized fluorescence spectra of Er/Yb:LBGW crystal excited by 521 nm radiation at room temperature.

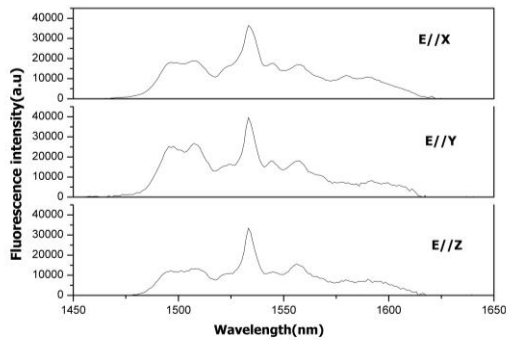


Fig. 4. Polarized fluorescence spectra of Er/Yb:LBGW crystal excited by 980 nm radiation at room temperature.

### 3.3 Up-conversion fluorescence under 980 nm excitation

Fig. 5 shows the non-polarized up-conversion fluorescence spectra of Er/Yb:LBGW crystals under excitation of 980 nm LD (power~0.9W). Three fluorescence emission bands at ~531, 552 and 650 nm were observed, which correspond to the  $^2H_{11/2} \rightarrow ^4I_{15/2}$ ,  $^4S_{3/2} \rightarrow ^4I_{15/2}$  and  $^4F_{9/2} \rightarrow ^4I_{15/2}$  transitions of  $Er^{3+}$  ion, respectively. The dependence of up-conversion fluorescence intensity for Er/Yb:LBGW on the excitation power at 980 nm is shown in Fig. 7. The relation between the up-conversion fluorescence intensity ( $I_{up}$ ) and the incident pump power ( $P_{pump}$ ) according to the following relation [23]

$$I_{up} \propto (P_{pump})^n \quad (16)$$

where  $n$  is the number of photon involved in the up-conversion process. It can be found that the slopes of the green fluorescence (530 nm, 552 nm) are 2.01 and 1.96, and the slope of the red fluorescence (656 nm) is 1.95 (see Fig. 6), which indicates that these three up-conversion fluorescence bands are due to a two-photon up-conversion process. Fig. 7 shows the energy level diagrams of  $Er^{3+}$  and  $Yb^{3+}$  ions, as well as the green and red up-conversion mechanisms in Er/Yb:LBGW crystal. Two different mechanisms,  $Er^{3+}$  excited state absorption (ESA) and Yb- $Er$  energy transfer (ET) may exist in the up-conversion process [24, 25].

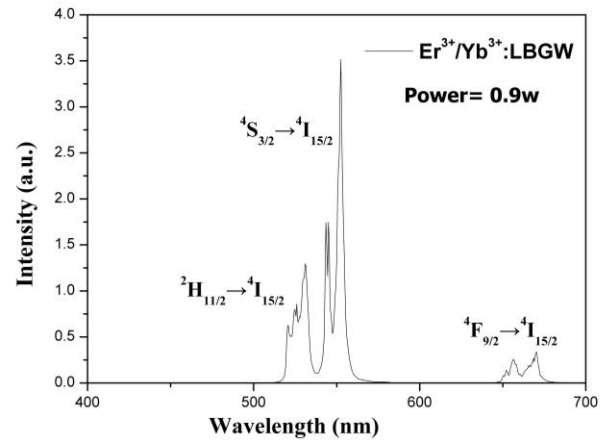


Fig. 5. Non-polarized up-conversion spectra of Er/Yb:LBGW crystal excited by 980 nm radiation at room temperature.

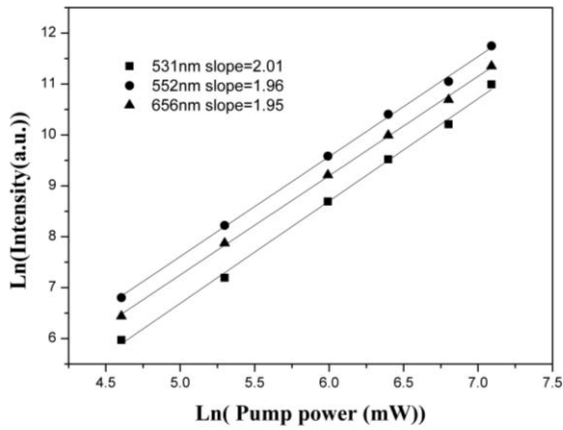


Fig. 6. In-ln plots of the integrated emission intensities versus excitation power for  $\text{Er}/\text{Yb}:\text{LBGW}$  crystal.

For the  $\text{Er}^{3+}/\text{Yb}^{3+}$  doped crystals, the ET process is dominant because of the large absorption cross section around 980 nm of  $\text{Yb}^{3+}$  ions [3], and ESA is a single ion

process, it is appropriate for up-conversion single-doped lasers. The  $\text{Er}^{3+}$  ions are firstly excited from ground state to the excited state by ground state absorption (GSA) or energy transfer processes. Secondly, most  $\text{Er}^{3+}$  ions at the  $^4\text{I}_{11/2}$  level are promoted up to the  $^4\text{F}_{7/2}$  level by ET process or ESA process (Fig. 7). The ions at the  $^4\text{F}_{7/2}$  ( $\text{Er}^{3+}$ ) relaxed to the lower level  $^2\text{H}_{11/2}/^4\text{S}_{3/2}/^4\text{F}_{9/2}$  through a nonradiative transition. When the  $\text{Er}^{3+}$  ions at the  $^2\text{H}_{11/2}$  and  $^4\text{S}_{3/2}$  level transitioned to the ground state, it produced 530 and 552 nm green fluorescence, respectively. Because the lifetime of the  $^4\text{S}_{3/2}$  level is longer than that of the  $^2\text{H}_{11/2}$  level, more ions would be populated at the  $^4\text{S}_{3/2}$  level. As a consequence, the intensity of green fluorescence 552 nm is stronger than that of 530nm. Furthermore, the ions at  $^4\text{I}_{11/2}$  level relax to  $^4\text{I}_{13/2}$  through nonradiative transition, then they excited to  $^4\text{F}_{9/2}$  level through ESA or ET process (Fig. 8). When the  $\text{Er}^{3+}$  ions at the  $^4\text{F}_{9/2}$  levels transitioned to the ground state, it produced 656 nm red fluorescence.

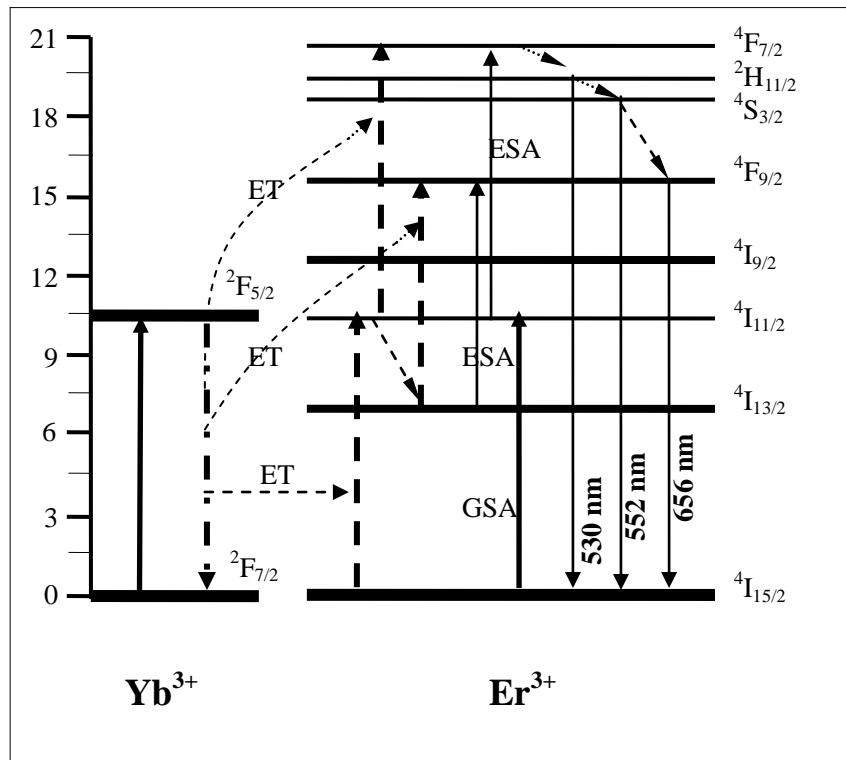


Fig. 7. Transition mechanisms and simplified energy levels of  $\text{Er}/\text{Yb}:\text{LBGW}$  crystal.

#### 4. Conclusions

$\text{Er}/\text{Yb}:\text{LBGW}$  crystal was grown by the TSSG method from a flux of  $\text{Li}_2\text{WO}_4$ . Based on the Judd-Ofelt theory the effective oscillator strength parameters of the  $\text{Er}^{3+}$  in

$\text{Er}/\text{Yb}:\text{LBGW}$  crystal were obtained:  $\Omega_2^{\text{eff}}=8.59\times 10^{-20}$   $\text{cm}^2$ ,  $\Omega_4^{\text{eff}}=1.87\times 10^{-20}$   $\text{cm}^2$  and  $\Omega_6^{\text{eff}}=0.25\times 10^{-20}$   $\text{cm}^2$ . The peak stimulated emission cross-section of the  $^4\text{I}_{13/2}\rightarrow^4\text{I}_{15/2}$  transition of  $\text{Er}^{3+}$  ion in  $\text{Er}/\text{Yb}:\text{LBGW}$  crystal for the E//Y polarization is  $0.61\times 10^{-20}$   $\text{cm}^2$  at  $1.5\mu\text{m}$ , which

is comparable to those reported Er<sup>3+</sup>-doped materials. The room-temperature up-conversion fluorescence spectra and mechanism were investigated. Three visible fluorescence bands at ~531, 552 and 650 nm, which correspond to the Er<sup>3+</sup> ion transitions of <sup>2</sup>H<sub>11/2</sub>→<sup>4</sup>I<sub>15/2</sub>, <sup>4</sup>S<sub>3/2</sub>→<sup>4</sup>I<sub>15/2</sub>, and <sup>4</sup>F<sub>9/2</sub>→<sup>4</sup>I<sub>15/2</sub> transitions, were observed. The dependence of up-conversion fluorescence intensity for Er/Yb:LBGW on the excitation power indicates that these three up-conversion fluorescence bands are due to a two-photon up-conversion process. The spectroscopic analysis reveals that Er/Yb:LBGW crystal may become a potential candidate for solid-state laser gain medium material.

### Acknowledgements

This work is supported by the National Natural Science Foundation of China (No. 61108054) and the National Natural Science Foundation of Fujian Province (No. 2011J01376), respectively.

### References

- [1] G. A. Kumar, *J. Appl. Phys.* **95**, 3243 (2004).
- [2] N. A. Tolstik, V. E. Kisel, N. V. Kuleshov, V. V. Maltsev, N. I. Leonyuk, *Appl. Phys. B* **97**, 357 (2009).
- [3] V. Singh, V. K. Rai, K. Al-Shamery, J. Nordmann, M. Haase, *J. Lumin.* **131**, 2679 (2011).
- [4] D. Zhao, Z. Hu, Z. Lin, G. Wang, *J. Cryst. Growth* **277**, 401 (2005).
- [5] T. Sanamyan, M. Kanskar, Y. Xiao, D. Kedlaya, M. Dubinskii, *Opt. Soc. Am.* **19**, 1082 (2011).
- [6] Z. Mierczyk, M. Kwasny, K. Kopczynski, A. Gietka, T. Lukaszewicz, Z. Frukacz, J. Kisielewski, R. Frukacz, J. Kisielewski, R. Stepien, K. Jedrzejek, *J. Alloys Compd.* **300**, 398 (2000).
- [7] R. Guo, Y. Wu, P. Fu, F. Jing, *Chem. Phys. Lett.* **416**, 133 (2005).
- [8] D. Garbuzov, I. Kudryashov, M. Dubinskii, *Appl. Phys. Lett.* **87**, 121101 (2005).
- [9] N. A. Tolstik, A. E. Troshin, S. V. Kurilchik, V. E. Kisel, N. V. Kuleshov, V. N. Matrosov, T. A. Matrosova, M. I. Kupchenko, *Appl. Phys. B* **86**, 275 (2006).
- [10] B. Wei, Z. B. Lin, G. F. Wang, *J. Cryst. Growth* **295**, 241 (2006).
- [11] H. Li, L. Z. Zhang, G. F. Wang, *J. Alloys Compd.* **478**, 484 (2009).
- [12] H. Li, G. F. Wang, L. Z. Zhang, Y. S. Huang, G. F. Wang, *CrystEngComm*, **12**, 1307 (2010).
- [13] B. R. Judd, *Phys. Rev.* **127**, 750 (1962).
- [14] G. S. Ofelt, *J. Chem. Phys.* **37**, 511 (1962).
- [15] X. Y. Huang, Z. B. Lin, L. Z. Zhang, G. F. Wang, *Mater. Res. Innovat.* **12**, 94 (2008).
- [16] B. Wei, L. Z. Zhang, Z. B. Lin, G. F. Wang, *Mater. Res. Innovat.* **11**, 154 (2007).
- [17] F. Song, L. Han, H. Tan, J. Su, J. Yang, J.-g. Tian, G.-y. Zhang, Z.-x. Cheng, H.-c. Chen, *Opt. Commun.* **259**, 179 (2006).
- [18] W. T. Carnall, P. R. Fields, B.G. Wybourne, *J. Chem. Phys.* **42**, 3797 (1965).
- [19] M. J. Weber, *Phys. Rev.* **157**, 262 (1967).
- [20] W. Zhao, W. W. Zhou, M. J. Song, G. F. Wang, J. M. Du, H. J. Yu, *J. Optoelectron. Adv. Mater - Rapid Commun.* **5**, 49 (2011).
- [21] B. F. Aull, H. P. Jenssen, *IEEE J. Quantum Electron.* **QE-18**, 925 (1982).
- [22] H. Stange, K. Petermann, E. W. D. G. Huber, *Appl. Phys. B* **49**, 269 (1989).
- [23] L. Li, Z. Zhou, L. Feng, H. Li, Y. Wu, *J. Alloys Compd.* **509**, 6457 (2011).
- [24] M.-F. Joubert, *Opt. Mater.* **11**, 181 (1999).
- [25] X. Y. Huang, W. Zhao, G. F. Wang, X. X. Li, Q. M. Yu, *J. Alloys Compd.* **509**, 6578 (2011).

\*Corresponding author: wgf@ms.fjirsm.ac.cn